Journal of Zhejiang University-SCIENCE B (Biomedicine & Biotechnology)
ISSN 1673-1581 (Print); ISSN 1862-1783 (Online)
www.zju.edu.cn/jzus; www.springerlink.com
E-mail: jzus@zju.edu.cn

Influence of heat stress on leaf ultrastructure, photosynthetic performance, and ascorbate peroxidase gene expression of two pear cultivars (*Pyrus pyrifolia*)*

Dong-feng LIU[1], Dong ZHANG[2], Guo-qin LIU[1], Sayed HUSSAIN[1], Yuan-wen TENG†‡[1]

([1]*State Agricultural Ministry Key Laboratory of Horticultural Plant Growth, Development and Quality Improvement, Department of Horticulture, Zhejiang University, Hangzhou 310058, China*)

([2]*College of Horticulture, Northwest A&F University, Yangling 712100, China*)

†E-mail: ywteng@zju.edu.cn

Received Mar. 27, 2013; Revision accepted July 1, 2013; Crosschecked Nov. 5, 2013

Abstract: Plants encounter a variety of stresses in natural environments. One-year-old pot-grown trees of pear (*Pyrus pyrifolia* Nakai cv. Cuiguan and Wonhwang) were exposed to two heat stress regimes. Under constant short-term heat stress, chloroplasts and mitochondria were visibly damaged. Relative chlorophyll content and maximum photochemical efficiency of photosystem II were significantly decreased, which indicated that the leaf photosynthetic capability declined. Under chronic heat stress, mesophyll cell ultrastructure was not obviously damaged, but leaf photosynthetic capability was still restrained. As chronic heat stress was a simulation of the natural environment in summer, further study of the responses under this stress regime was undertaken. Ascorbate peroxidase (APX) activity was increased in 'Cuiguan', but not in 'Wonhwang'. Inducible expression of *PpAPX* genes in the cytoplasm, chloroplasts and peroxisomes was consistent with increased APX activity in 'Cuiguan', whereas only weak induction of *PpAPX* genes was observed in 'Wonhwang'. The isoenzymes cytosolic APX1 (cAPX1) and stromal APX (sAPX) were confirmed to be localized in the cytoplasm and chloroplasts, respectively.

Key words: Pear, Ultrastructure, Ascorbate peroxidase, Subcellular localization, Synergistic effect
doi:10.1631/jzus.B1300094 **Document code:** A **CLC number:** Q37

1 Introduction

Chinese sand pear (*Pyrus pyrifolia* Nakai) is an economically important fruit species and is cultivated widely in China. In the context of global climate change, increasing frequency and duration of extremely high temperature have exerted a negative impact on fruit production in the pear industry via effects such as leaf scorch, decreased flower bud formation, and abnormal flowering (Glenn *et al.*, 2002; Li and Cheng, 2009; Huang *et al.*, 2010; Wang *et al.*, 2011). As sessile organisms, plants have evolved a powerful mechanism for adaptation to extreme temperature (Bohnert *et al.*, 1995). The antioxidant system is a universal and important protective pathway because almost all abiotic stresses generate reactive oxygen species (ROS) (Foyer *et al.*, 1994; Asada, 1999; Mittler *et al.*, 2004). Excess ROS can attack proteins, lipids, or nucleic acids, and ultimately lead to injury symptoms (Fridovich, 1998; Karpinski *et al.*, 1999; Vanderauwera *et al.*, 2011). Chloroplasts and mitochondria are the predominant sites of ROS generation because of their high concentration of oxygen and they are easily damaged under stress conditions (Mittler *et al.*, 2004; Asada, 2006). Hydrogen

‡ Corresponding author
* Project (No. nycytx-29) supported by the Earmarked Fund for the Modern Agro-industry Technology Research System, China

peroxide (H_2O_2) is considered extremely harmful among ROS because it is easily diffused and converted to ·OH (Bienert *et al.*, 2007). However, H_2O_2 also functions as a signal molecule in important physiological processes (Dat *et al.*, 2000; Mittler, 2002; Neill *et al.*, 2002; Vandenabeele *et al.*, 2003; Apel and Hirt, 2004; Mullineaux, 2006). H_2O_2 induces expression of small heat shock protein genes and activates heat shock transcription factors under heat stress (Volkov *et al.*, 2006). Moreover, H_2O_2 arouses defense responses in unstressed regions as a systemic signal (Karpinski *et al.*, 1999). Thus, dissipation of excess H_2O_2 is essential owing to its dual roles.

In contrast to annuals, perennial fruit trees have a more complex branching structure, in which the shading of leaves may be beneficial for stress adaptation, but high leaf density also potentially aggravates stress. In our previous study, the different responses of the *P. pyrifolia* cultivars 'Cuiguan' and 'Wonhwang' to environmental stress were reported (Ji *et al.*, 2012). In the present study, the two cultivars were chosen to study their thermal performance under high temperature treatment.

2 Materials and methods

2.1 Plant materials and treatments

2.1.1 Experiment 1: constant short-term heat stress regime

One-year-old *P. pyrifolia* cv. Cuiguan (CG) and Wonhwang (WH) trees were planted in 53-L pots and tended in accordance with standard fertilization and pest-control practices outdoors. In July, six trees of each cultivar were transferred to a growth chamber for constant short-term heat stress treatment. Three trees of each cultivar were grown under a constant high temperature of 40 °C for 2 d and three trees were cultivated at 27 °C (the control). The illumination was 75% natural sunlight and relative humidity was 60%–70%. After treatment for 2 d, leaves were harvested for observation of the mesophyll cell ultrastructure. Relative chlorophyll content was measured with a SPAD meter (SPAD-502, Minolta, Japan), and maximum photosystem II (PSII) photochemical efficiency (the ratio of variable to maximum fluorescence, F_v/F_m) of leaves was measured before and at completion of short-term heat stress treatment.

2.1.2 Experiment 2: chronic heat stress regime

An additional six trees of each cultivar were selected for chronic heat stress treatment. Three trees of each cultivar were cultivated at 40 °C from 11:00 to 17:00 and at 27 °C for the remainder of the day, while three trees were grown at a constant temperature of 27 °C (the control). The other growing conditions were identical to those of Experiment 1. After treatment for 6 d, leaves were harvested for observation of the mesophyll cell ultrastructure, and all trees were transferred to field conditions for recovery. F_v/F_m was measured daily at 10:00 before the increase in temperature. On the last day of treatment, the net photosynthetic rate (P_n) was measured at 11:00 to evaluate the influence of chronic heat stress on leaf photosynthetic capacity. After recovery for 6 d in the field, P_n was measured again to evaluate the recovery capability of the photosynthetic apparatus. During chronic heat stress treatment, healthy leaves were sampled daily, frozen in liquid N_2, and stored at −80 °C for analyses of enzyme activity and gene expression.

2.2 Observation of mesophyll cell ultrastructure

Fresh leaves were sliced and fixed in 2.5% glutaraldehyde for 12 h at 4 °C. After washing in 100 mmol/L phosphate buffer (pH 7.0) and fixing in 1% (0.01 g/ml) osmium tetroxide, the leaf slices were dehydrated, embedded in Epon-812 resin and stained with uranyl acetate and lead citrate. Ultrathin sections (80 nm) were prepared and observed with a transmission electron microscope (JEOL, Japan) at 80 kV. The numbers of normal and deformed chloroplasts in Experiment 1 were counted in micrographs of 30 mesophyll cells.

2.3 Evaluation of leaf photosynthetic capacity

The F_v/F_m ratio was measured with a chlorophyll fluorometer (Walz, Germany). After dark adaptation for 20 min, three leaves were detached and transferred to room temperature for measurement. The measurement light intensity was 0.12 μmol/(m^2·s) for measurement of the dark-adapted minimum fluorescence yield (F_o) and a saturating pulse of 5000 μmol/(m^2·s) at 0.8 s intervals for measurement of the dark-adapted maximal fluorescence yield (F_m). The F_v/F_m ratio was calculated as $F_v/F_m=(F_m-F_o)/F_m$. P_n was measured with a Li-6400 photosynthesis system (Li-COR, USA); the measurement

parameters were 800 μmol/(m^2·s) light intensity and 400 μmol/mol CO_2. Relative chlorophyll content was measured with a SPAD-502 portable leaf greenness meter (Minolta, Japan).

2.4 Assay of lipid peroxidation content and ascorbate peroxidase activity

Malondialdehyde (MDA) content in leaf was determined with the method described by Heath and Packer (1968). Activity of ascorbate peroxidase (APX) was determined in accordance with the method described by Nakano and Asada (1981) with slight modification. Ground leaf tissue (0.5 g) was added to 100 mmol/L potassium phosphate buffer (pH 7.8) containing 2 mmol/L ethylenediaminetetraacetic acid disodium salt (EDTA), 5 mmol/L ascorbate, and 2% (0.02 g/ml) polyvinyl pyrrolidone, and then centrifuged at 14000×*g* for 10 min at 4 °C. Oxidation of ascorbate was initiated by addition of H_2O_2, and the absorbance at 290 nm was dynamically monitored for 1 min. One unit of APX activity was defined as an absorbance change of 0.01 per minute.

2.5 Gene clone and sequence analysis

Total RNA was extracted from CG leaves. Digested RNA treated with DNase I was reverse-transcribed using the Revert Aid™ First Strand cDNA Synthesis Kit (Fermentas, USA). Primers for cloning the *APX* gene (Table 1) were designed based on conserved regions or transcriptome data (Liu *et al*., 2012). After obtaining partial sequences, the flanking sequence was amplified by nest-polymerase chain reaction (PCR) using the SMART RACE cDNA Amplification Kit (Clontech, USA). Amino acid sequences were deduced with the online ORF Finder tool (http://www.ncbi.nlm.nih.gov/gorf/orfig.cgi). Nucleotide sequences of other plant *APX* genes (Panchuk *et al*., 2002; Teixeira *et al*., 2004; Najami *et al*., 2008; Sečenji *et al*., 2009) were retrieved from the National Center for Biotechnology Information (NCBI) databases. A dendrogram was constructed using the neighbor-joining method with MEGA 5.0 software. Bootstrap support values (from an analysis with 1000 replicates) were denoted at each node.

2.6 Subcellular localization of *PpcAPX1* and *PpsAPX*

The open reading frames with a mutated terminator for *PpcAPX1* and *PpsAPX* were cloned into the pMD18T-vector (TaKaRa, Japan) using primers with restriction enzyme sites and a protective base pair for *Kpn*I and *Bam*HI at the 5′ terminus. The primers are listed in Table 1. Clone products and the pCHF3-GFP vector were double-digested by *Kpn*I and *Bam*HI (TaKaRa, Japan). The recombinant plasmid was transformed into *Agrobacterium tumefaciens* strain EHA105 and transiently expressed in *Nicotiana benthamiana* (Sparkes *et al*., 2006). Infiltrated leaves were observed with a confocal laser scanning microscope (Zeiss, Germany). Excitation and emission

Table 1 Primers used for cloning, quantification, and subsellular localization of *PpAPX*

Gene	Primer (5′–3′)	Product size (bp)
Gene cloning		
PpcAPX1	Forward: ACATGGGGCACTCACTCTCC	1070
	Reverse: GCTTTATTCAATCTACAAGG	
PpcAPX2	Forward: ACATGGGGGTGCCACTCCATAG	1070
	Reverse: GAAGTGAAAATTACAGTAT	
PpcAPX3	Forward: TTAGATATCCATTTTGATGTG	1163
	Reverse: ACCTCTGACATTACATTCGT	
PppAPX	Forward: AAAACCACATCTGTCCAGCT	1155
	Reverse: CATGTCACTATGTCCGTCGT	
PpsAPX	Forward: ATCTGTCCATTTTCCAAATC	1577
	Reverse: TTGATAGCAATGTAATTCTCAT	
PptAPX	Forward: GCCCCACCATTGGGGTGGAA	1009
	Reverse: GGAAATGCAACATTACAAGG	
Quantification		
PpcAPX1	Forward: GGAGAACCAAAAGGGATGATG	204
	Reverse: GAATTGAAAATGACGGCTTTA	
PpcAPX2	Forward: CGCGCCTTGCTTTTGTTT	192
	Reverse: TAATACTGTAATTTTCACTTC	
PpcAPX3	Forward: TCCAGTCTTTCGCCCTCT	132
	Reverse: CTACAAATCACAATCCCTTA	
PppAPX	Forward: CGATACTGGCACAAGGAG	179
	Reverse: ATTCGTAAGGGATCAAGG	
PpsAPX	Forward: CATGCTTACTTGTGCCATCTG	206
	Reverse: AGAGGCTTATCTGGGCTTCC	
PptAPX	Forward: CTTTGGGCCAACAAATCAAT	201
	Reverse: GACGCAGTTTTGAAGAGATGC	
Subcellular localization		
PpcAPX1	Forward: GGGGTACCACATGGGGCA CTCACTCTCCATCGC	833
	Reverse: CGGGATCCGGCCTCAGCA AACCCGAGCTCAGAG	
PpsAPX	Forward: GGGGTACCAGCCATCTGTC CATTTTCCA	1233
	Reverse: CGGGATCCCTCCTTGCCAG ATGAGTATTTGGC	

wavelengths for the green fluorescence protein (GFP) were 488 nm and 505–530 nm, respectively. Images were processed with ZEN 2009 Light Edition software.

2.7 Quantitative real-time PCR

The primers used for quantitative real-time PCR (qRT-PCR) (Table 1) were designed on the basis of the 3′-untranslated region sequence. The product length was no more than 210 bp. An identical product was amplified in both pear cultivars, primer specificity was confirmed by obtaining a single melting-curve peak, and a single band was visualized with agarose gel electrophoresis. The total reaction volume for qRT-PCR was 15 μl, which comprised 7.5 μl SYBR Green PCR Supermix (TaKaRa, Japan), 0.5 μl each primer, 1 μl of 1:10 (v/v) diluted cDNA, and 5.5 μl ddH_2O_2. The amplification procedure comprised denaturation for 5 min at 94 °C, 45 cycles of 94 °C for 10 s and 60 °C for 30 s, and was conducted with a Roche LightCycler® 480 (Roche, Germany). *PpActin* (JN684184) was used as a housekeeping gene (Yu *et al*., 2012). Relative gene expression levels were calculated by the $2^{-\Delta\Delta C_T}$ method (Livak and Schmittgen, 2001).

2.8 Statistical analysis

Statistical analyses were performed using the least-significant difference (LSD) test at the $P<0.05$ significance level with SPSS 13.0 software.

3 Results

3.1 Effect of constant short-term heat stress on mesophyll cell ultrastructure and photosynthetic performance of leaves

Damage from constant short-term heat stress was observed in chloroplasts, mitochondria, and the nucleus of mesophyll cells. In non-stressed cells, chloroplasts were elliptic or spindle-shaped, contained plump white starch grains, and were located adjacent to the cell wall. In the nucleus, chromatin was equally dispersed without aggregation. Under high-power magnification, stacked thylakoids and rod-like mitochondrial cristae were evident (Figs. 1 and 2). After constant short-term heat stress, the chloroplasts were swollen and were displaced from the cell wall. In the nucleus, chromatin was agglutinated with heterochromatin. Under high-power magnification, the thylakoids and mitochondrial cristae were swollen, ruptured, or had disappeared (Figs. 1 and 2). The percentage of deformed chloroplasts in heat-stressed leaves was 55% in CG and 57% in WH (Table 2). The relative chlorophyll content and F_v/F_m decreased after constant short-term heat stress in both cultivars (Fig. 3).

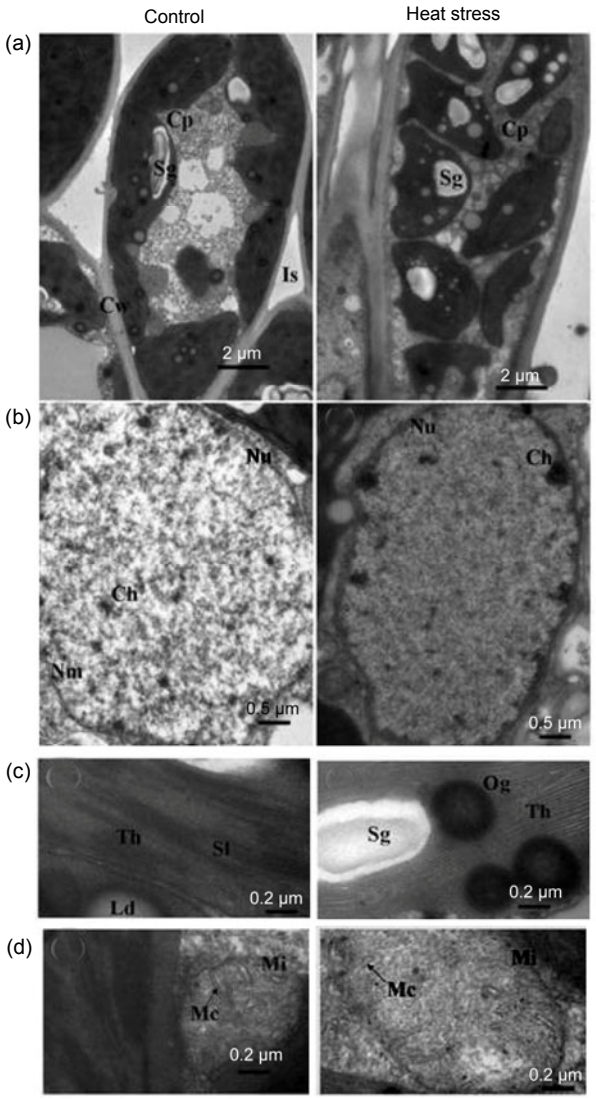

Fig. 1 Influence of constant short-term heat stress on mesophyll cell ultrastructure of 'Cuiguan'
Performances of cells (a), nucleus (b), thylakoids (c), and mitochondrion (d) under control or heat stress conditions. Cw: cell wall; Nu: nucleus; Cp: chloroplast; Th: thylakoids; Sl: stroma lamellae; Nm: nuclear membrane; Ch: chromatin; Sg: starch grain; Og: osmiophilic globule; Ld: lipid droplet; Is: intercellular space; Mi: mitochondrion; Mc: mitochondrial cristae

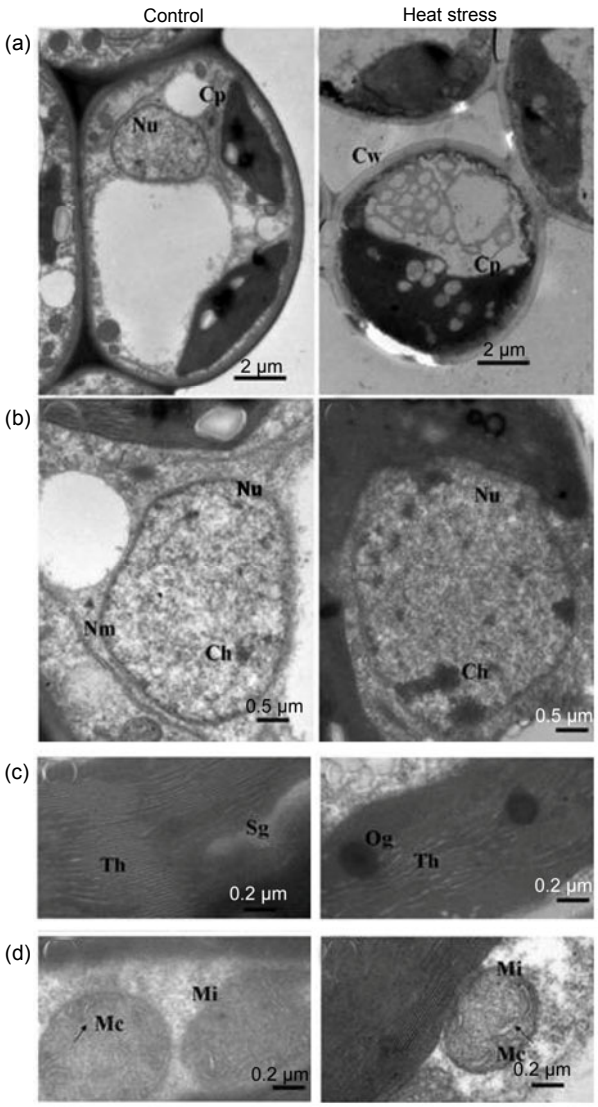

Fig. 2 Influence of constant short-term heat stress on mesophyll cell ultrastructure of 'Wonhwang'

Performances of cells (a), nucleus (b), thylakoids (c), and mitochondrion (d) under control or heat stress conditions. All the abbreviations are the same as those illustrated in Fig. 1

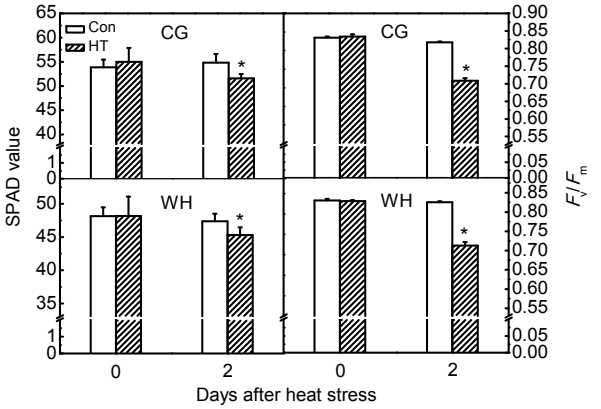

Fig. 3 Influence of constant short-term heat stress on relative chlorophyll contents and maximum photochemical efficiencies of PSII (F_v/F_m) of 'Cuiguan' (CG) and 'Wonhwang' (WH) leaves

The values represent the mean of three experiments± standard error. Asterisks indicate a significant difference between the control (Con) and heat stress treatment (HT) at $P<0.05$

Table 2 Integrity of chloroplast in leaves of 'Cuiguan' and 'Wonhwang' under constant short-term heat stress

Treatment	Cuiguan		Wonhwang	
	Normal	Deformed	Normal	Deformed
Control	0.91±0.02	0.09±0.02	0.86±0.01	0.14±0.01
Heat stress	0.45±0.06	0.55±0.06	0.43±0.02	0.57±0.02
P value	<0.01	<0.01	<0.01	<0.01

3.2 Effect of chronic heat stress on mesophyll cell ultrastructure and photosynthetic performance of leaves

Damage from chronic heat stress on mesophyll cell ultrastructure was less severe than that induced by constant heat stress in both cultivars. Chloroplasts, mitochondria, and the nucleus showed a normal appearance after chronic heat stress (Figs. 4 and 5). However, photosynthetic performance was affected by chronic heat stress. F_v/F_m of healthy leaves decreased but was still above 0.82 (Fig. 6), whereas F_v/F_m of visibly damaged leaves was less than 0.2 (data not shown). P_n significantly decreased at completion of chronic heat stress treatment but, after 6 d of recovery in the field, P_n of treated trees increased and attained a similar level to that of control trees (Fig. 6). However, after 6 d recovery in the field, P_n of control trees was significantly lower than that recorded in the growth chamber, which may be due to suboptimal conditions during the hot summer.

3.3 Influence of chronic heat stress on lipid peroxidation and APX activity

After chronic heat-stress treatment, MDA content in the leaves significantly increased in both cultivars, and was higher in WH than in CG both before and after heat stress treatment (Fig. 7). The percentage increase in CG (24%) was lower than that in WH (28%). Activity of APX was significantly increased in

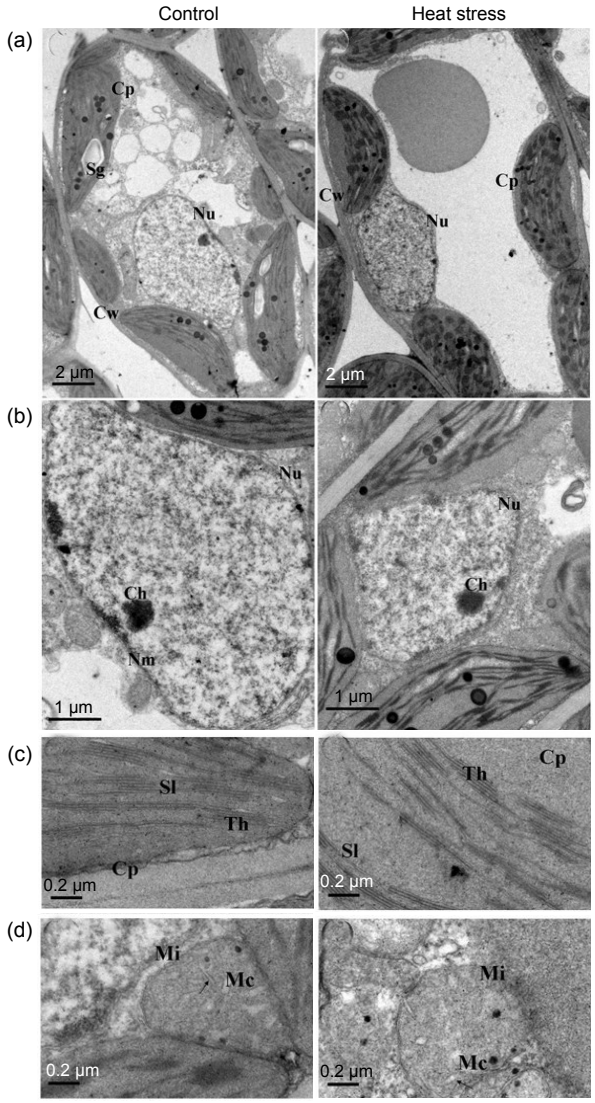

Fig. 4 Influence of chronic heat stress on mesophyll cell ultrastructure of 'Cuiguan'

Performances of cells (a), nucleus (b), thylakoids (c), and mitochondrion (d) under control or heat stress conditions. All the abbreviations are the same as those illustrated in Fig. 1

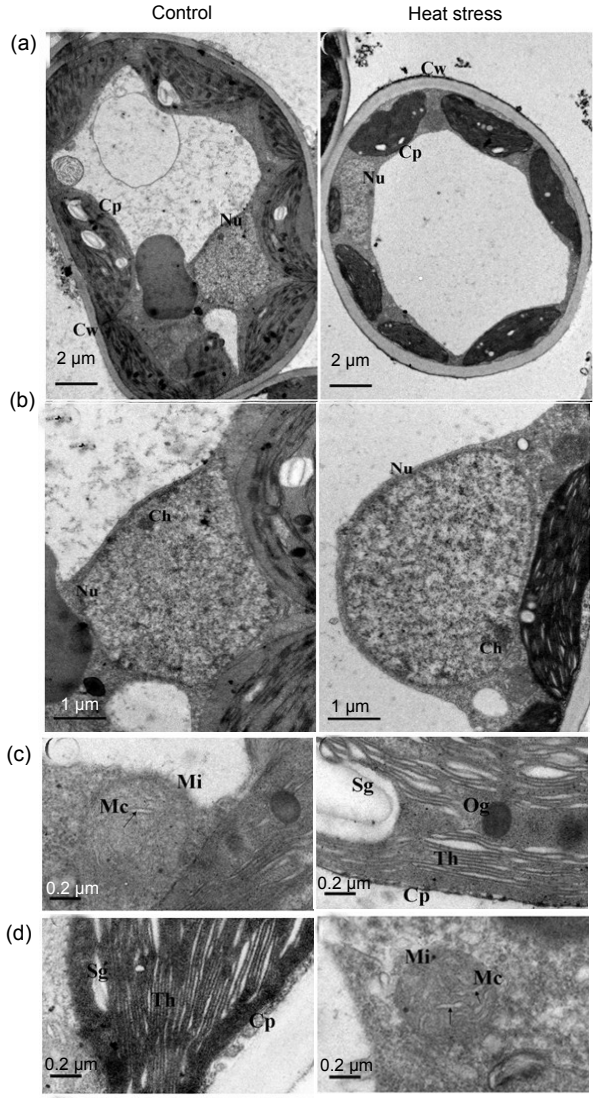

Fig. 5 Influence of chronic heat stress on mesophyll cell ultrastructure of 'Wonhwang'

Performances of cells (a), nucleus (b), thylakoids (c), and mitochondrion (d) under control or heat stress conditions. All the abbreviations are the same as those illustrated in Fig. 1

CG at 4 and 5 d of chronic heat stress treatment, whereas no significant change in APX activity was observed in WH (Fig. 7).

3.4 Isolation, characterization, and subcellular localization of *PpAPX* genes

Six *PpAPX* genes were isolated from CG leaves and were designated as *PpcAPX1* (JX104652), *PpcAPX2* (JX104653), *PpcAPX3* (JX104654), *PppAPX4* (JX104655), *PpsAPX* (JX104656), and *PptAPX* (JX104657), respectively. The deduced protein was putatively localized in the cytoplasm, peroxisomes, or chloroplasts by PSORT Server (http://psort.hgc.jp/) and TargetP 1.1 Server (http://www.cbs.dtu.dk/services/TargetP/). In the neighbor-joining dendrogram, the genes were grouped into three main clusters, consistent with their subcellular localization (Fig. 8). The cytosolic APXs shared a high level of sequence identity (83%), and identities between subgroups were lower (32%–67%). The identity between cytosolic and peroxisomal APXs was higher than that between the chloroplastic APX

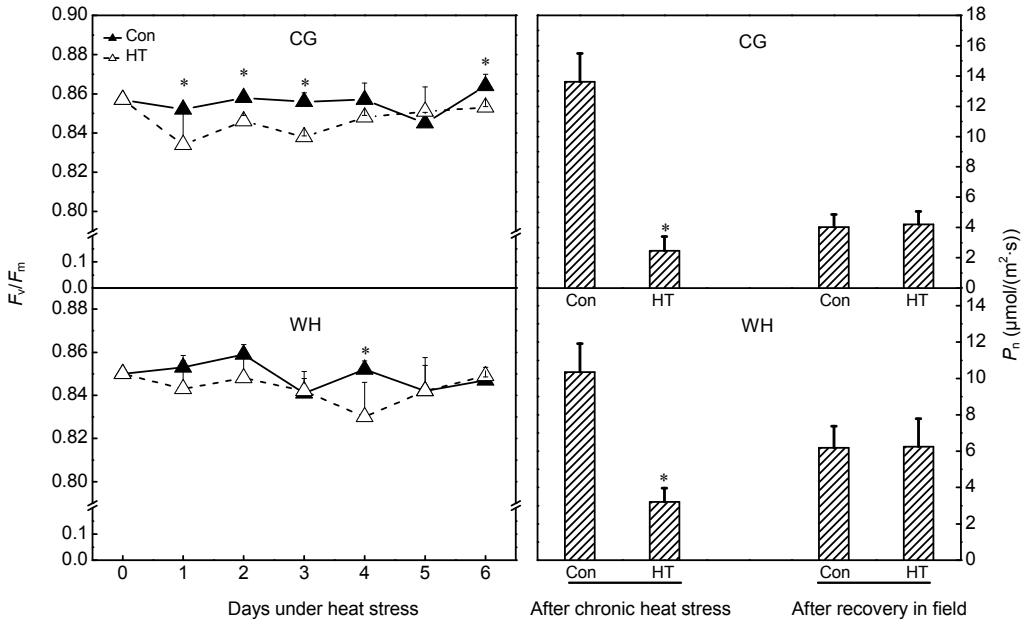

Fig. 6 Influence of chronic heat stress on maximum photochemical efficiencies of PSII (F_v/F_m) and net photosynthetic rates (P_n) of 'Cuiguan' (CG) and 'Wonhwang' (WH) leaves

The values represent the mean of three experiments±standard error. Asterisks indicate a significant difference between the control (Con) and heat stress treatment (HT) at $P<0.05$

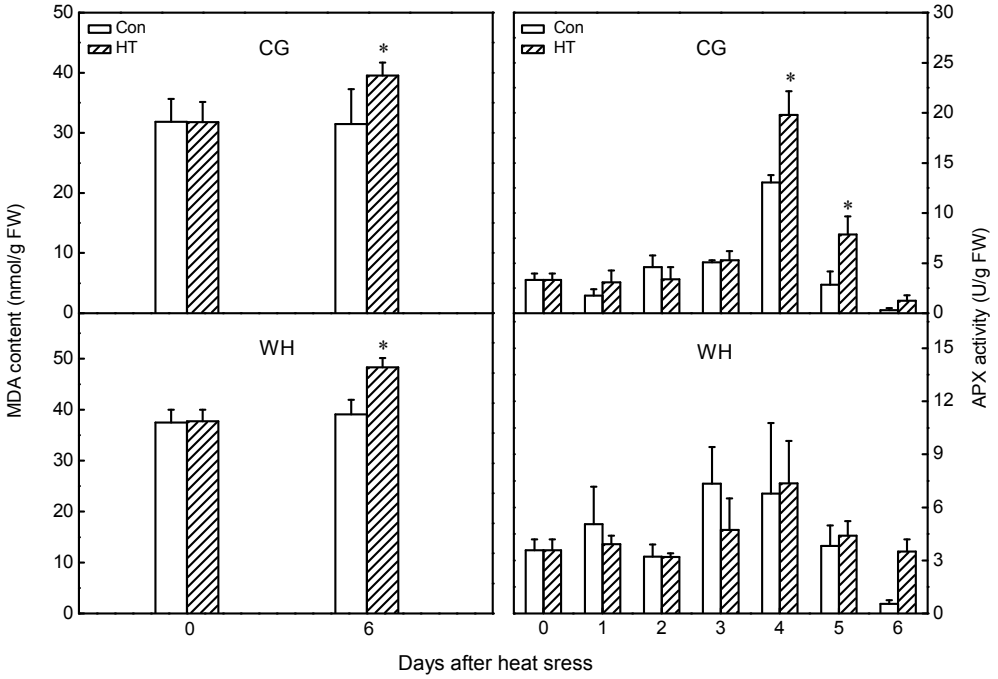

Fig. 7 Influence of chronic heat stress on malondialdehyde (MDA) contents and ascorbate peroxidase (APX) activities of 'Cuiguan' (CG) and 'Wonhwang' (WH) leaves

The values represent the mean of three experiments±standard error. Asterisks indicate a significant difference between the control (Con) and heat stress treatment (HT) at $P<0.05$

and either peroxisomal or cytosolic APX. The peroxisomal APX isoenzyme was predicted to have a transmembrane helix at the C-terminus, and the 22-amino-acid core region of the transmembrane helix was located from positions 260 to 281 in the amino acid sequence, as predicted by the TMpred tool (http://www.ch.embnet.org/software/TMPRED_form.html). The stromal APX isoenzyme was predicted to have a chloroplast transit peptide (87 amino acids in length) at the N-terminus with the ChloroP Server (http://www.cbs.dtu.dk/services/ChloroP/).

Subcellular localizations of the cytosolic and chloroplastic isoenzymes (cAPX1 and sAPX, respectively) were verified in vivo by transient expression of fluorescent fusion proteins (Fig. 9). The differential interference contrast image showed that fluorescence of the GFP-cAPX1 fusion protein was distributed in the cytoplasm around the cell periphery (Figs. 9a–9c). Fluorescence of the GFP-sAPX fusion protein was detected in spherical spots distributed throughout the cytoplasm, and the spherical chloroplasts were discernible on the basis of the red autofluorescence of chlorophyll; the merged image confirmed that the GFP-sAPX fusion protein was specifically localized in chloroplasts (Figs. 9d–9f). However, because of the magnification limit of the confocal microscope, the stromal location of the GFP-sAPX fusion protein in the chloroplasts could not be resolved.

3.5 Effect of chronic heat stress on *PpAPX* genes transcription level

Given the observed differences in APX activity, expression analysis of *PpAPX* genes under chronic heat stress was investigated. In CG, expression of *PpcAPX1* was more stable than that of the other two cytosolic *APX* genes. Expression of *PpcAPX2* was

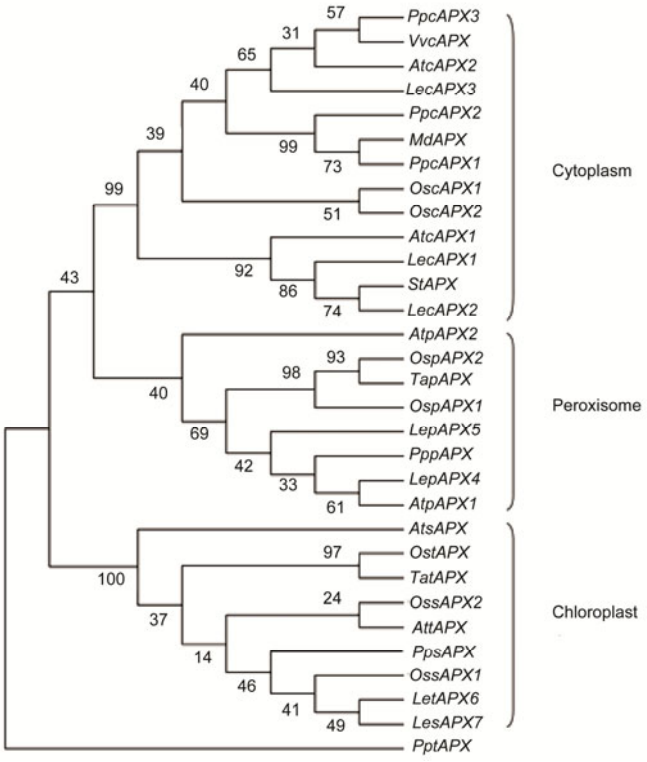

Fig. 8 Phylogenetic relationships of ascorbate peroxidase (APX) isoenzymes from different plant species
At: *Arabidopsis thaliana* (*cAPX1*: NM_001123772; *cAPX2*: NM_111798; *pAPX1*: NM_119666; *pAPX2*: NM_119763; *sAPX*: NM_001084887; *tAPX*: NM_106398); Os: *Oryza sativa* (*cAPX1*: D45423; *cAPX2*: AB053297; *pAPX1*: AK070842; *pAPX2*: 3AY382617; *sAPX1*: AK061107; *sAPX2*: AK103344; *tAPX*: AB114856); Le: *Lycopersicon esculentum* (*cAPX1*: DQ096286; *cAPX2*: DQ096287; *cAPX3*: DQ131129; *pAPX4*: ABA10744; *pAPX5*: ABA10745; *tAPX6*: DQ131132; *sAPX7*: DQ131133); Ta: *Triticum aestivum* (*tAPX*: AY513262; *pAPX*: EF555121); St: *Solanum tuberosum* (AB041343); Md: *Malus domestica* (EF528482); Vv: *Vitis vinifera* (*cAPX*: EU280159); Pp: *Pyrus pyrifolia* (*cAPX1*: JX104652; *cAPX2*: JX104653; *cAPX3*: JX104654; *pAPX*: JX104655; *sAPX*: JX104656; *tAPX*: JX104657)

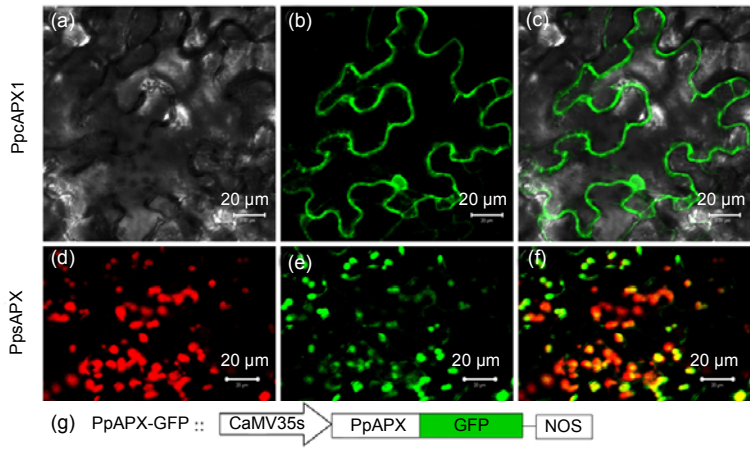

Fig. 9 Subcellular localization of APX-GFP fusion protein in *Nicotiana benthamiana* leaves

Confocal laser micrographs of tobacco cells expressing GFP-PpcAPX1 (a–c) and GFP-PpsAPX (d–f) fusion proteins. (a) Differential interference contrast image; (b, e) GFP fluorescence; (c) Merged image of (a) and (b); (d) Chlorophyll autofluorescence; (f) Merged image of (d) and (e); (g) Schematic representation of the T-DNA construction

immediately induced after 1 d of chronic heat stress and was maintained for 5 d, whereas significant induction of *PpcAPX3* was delayed until the 3rd day and thereafter was maintained for 3 d. Inductions of both *PpcAPX2* and *PpcAPX3* were weakened with increasing duration of chronic heat stress (Fig. 10a). Compared to that of CG, expressions of the three cytosolic *PpcAPX* genes in WH showed less marked up-regulation during chronic heat stress, and expression of *PpcAPX1* was inhibited (Fig. 10b).

Expression of APX isoenzymes localized in peroxisomes and chloroplasts also differed between CG and WH. *PppAPX*, *PpsAPX*, and *PptAPX* showed similar transcription trends in CG during chronic heat stress. The three *APX* genes were significantly induced at 3 d after heat stress, and thereafter maintained for 3 d (P<0.05). Thereafter, induction was weakened (Fig. 10a). In WH, the *PppAPX* transcript level was not affected by chronic heat stress. In chloroplasts, up-regulation of *PpsAPX* by 2.4-fold after 1 d of treatment and by 2.2-fold after 2 d of chronic heat stress was observed, but thereafter transcription was increasingly inhibited with continued chronic heat stress (Fig. 10b).

4 Discussion

Chloroplasts, mitochondria, and peroxisomes are the major ROS generation sites and are easily damaged under stress conditions in plants (Kratsch and Wise, 2000; Mittler *et al.*, 2004; Yamamoto *et al.*, 2008). Apparent ultrastructural changes were observed in mesophyll cells in response to constant short-term heat stress. Deformed chloroplasts, increased abundance of lipid droplets, swollen thylakoids and mitochondrial cristae, and condensed euchromatin were detected (Figs. 1 and 2). The percentage of damaged chloroplasts was 55% in CG and 57% in WH (Table 2), which indicated that the ultrastructure of mesophyll cells was severely damaged after only 2 d of constant heat stress.

Photosynthesis is the primary function of mesophyll cells. The photosynthetic apparatus is easily damaged by major ROS generation during primary photochemical reactions under environmental stresses. In chloroplasts, the D1 protein, which is a component of the PSII reaction center, is damaged by ROS (Yamamoto *et al.*, 2008). Therefore, maximum photochemical efficiency of PSII (F_v/F_m) is considered an indicator of plant stress status (Krause and Weis, 1984; Havaux, 1993). F_v/F_m was significantly decreased after constant heat stress (Fig. 3), which indicated that essential functions of the mesophyll cell were inhibited. Changes in mesophyll cell ultrastructure and photosynthetic performance after chronic heat stress differed from those observed in response to constant heat stress. Damage from chronic heat stress on the mesophyll cell ultrastructure was less severe than that induced by constant heat stress in both cultivars (Figs. 4 and 5). Photosynthetic performance also varied with the heat stress regime.

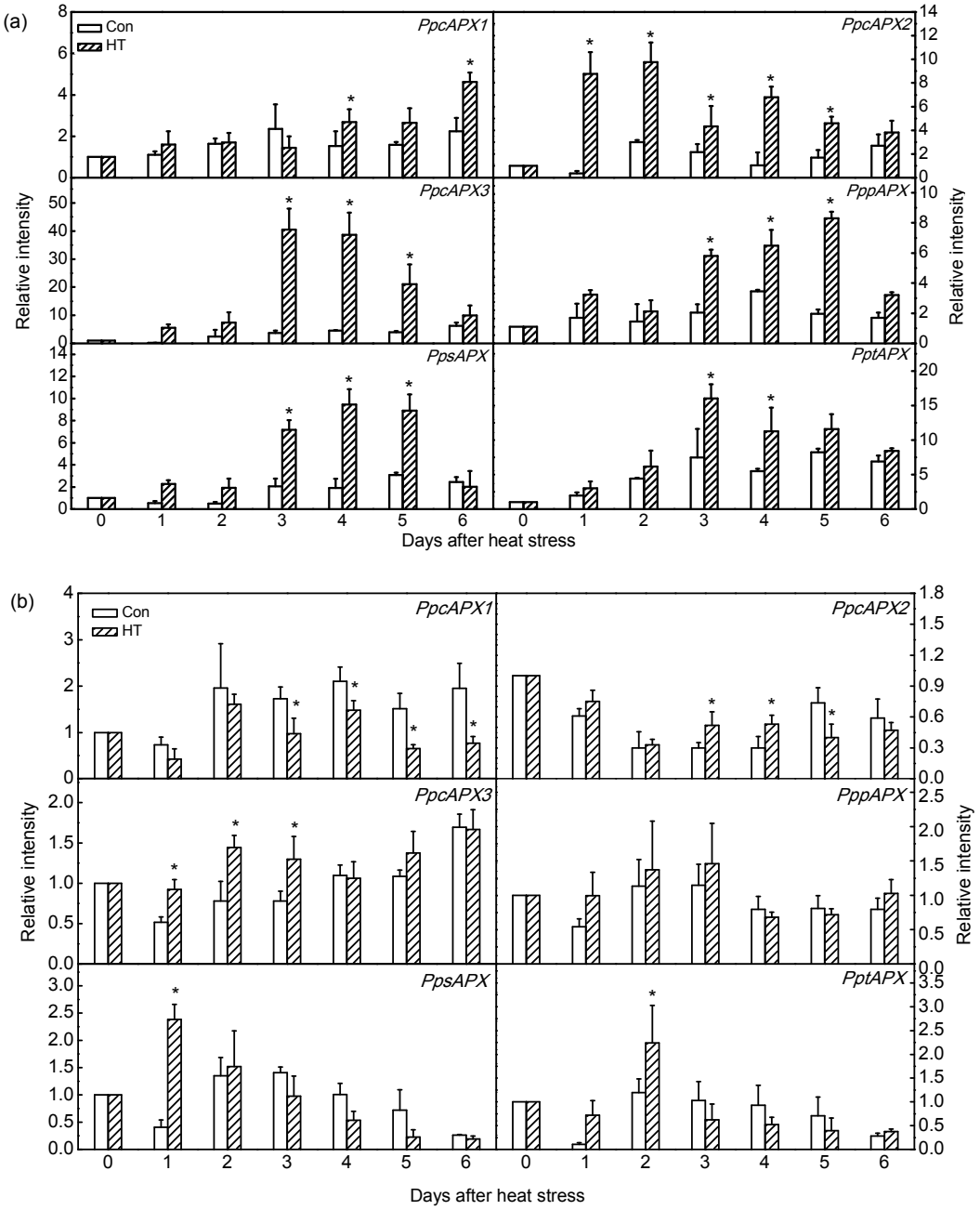

Fig. 10 Expression analysis of APX isoenzyme genes in 'Cuiguan' (a) and 'Wonhwang' (b) leaves under chronic heat stress
The values represent the mean of three experiments±standard error. Asterisks indicate a significant difference between the control (Con) and heat stress treatment (HT) at $P<0.05$

Under constant heat stress, F_v/F_m declined to nearly 0.7, whereas under chronic heat stress it decreased less markedly to 0.82 (Fig. 6). Previous studies have shown that a decrease in F_v/F_m is dependent on the stress regime and species. In cotton F_v/F_m was only affected if the temperature exceeded 40 °C, whereas in wheat F_v/F_m abruptly decreased at 35 °C (Law and Crafts-Brandner, 1999; Crafts-Brandner and Salvucci, 2002). In the present study, F_v/F_m was maintained above 0.82 under chronic heat stress (Fig. 6), which indicated that chronic heat stress did not severely damage the pear PSII, or the damaged PSII center was able to recover at a suitable night temperature. It was indicated that repair of the D1 protein in CG was

superior to that of WH at high temperature and strong light conditions (Ji *et al.*, 2012). The repair mechanism is rapid and efficient (Aro *et al.*, 2005). However, with increased duration of chronic heat stress, P_n significantly decreased in both cultivars (Fig. 6). After recovery under field conditions, the photosynthetic capacity of heat-stressed trees was partially restored, which indicated that stomatal limitation was the main reason for photosynthetic inhibition under chronic heat stress, because stomatal conductance and intercellular carbon dioxide concentration decreased under chronic heat stress (data not shown). However, P_n of control trees unexpectedly decreased after recovery (Fig. 6), which might be a result of unsuitable field conditions because the experiment was conducted during a hot summer.

APX is a key enzyme in the ascorbate-glutathione cycle, which plays a central role in scavenging H_2O_2 under stress conditions (Shigeoka *et al.*, 2002). APX is widely distributed in plants and eukaryotic algae, but the number and distribution of APX isoenyzmes are much more limited in algae than in higher plants (Ishikawa and Shigeoka, 2008). APX belongs to a multigenic family that is classified according to subcellular localization, e.g., cytoplasm, chloroplasts, mitochondria, and peroxisomes in higher plants (Mittler and Zilinskas, 1992; Jimenez *et al.*, 1997; Ishikawa *et al.*, 1998; Teixeira *et al.*, 2004; 2006). Six APX isoenzyme genes were isolated from *P. pyrifolia*, which were located in the cytoplasm, peroxisomes, and chloroplasts (Fig. 8). Sequence analysis showed that higher homology existed between the peroxisomal and cytosolic APXs than between chloroplastic and either peroxisomal or cytosolic APXs (Fig. 8). The peroxisomal APX was similar to the cytosolic APX except that the former contained a transmembrane helix at the C-terminus, which was consistent with the hypothesis that cytosolic and peroxisomal APXs diverged from chloroplastic APX (Teixeira *et al.*, 2004; Najami *et al.*, 2008). Chloroplastic APX isoenzyme genes are divided into two groups in plants. In the first group, stroma and thylakoid APXs are encoded by alternative splicing of one gene, as in spinach (Ishikawa *et al.*, 1997), whereas in the second group there are two individual genes for different isoenzymes (Teixeira *et al.*, 2004; Najami *et al.*, 2008). The two chloroplastic *APX* genes in *P. pyrifolia* belonged to the second group (Fig. 8). A transit signal was predicted to be present in the N-terminus of stroma APX. Its targeting function was confirmed in vivo (Fig. 9), but the transit signal in stroma APX also has a dual targeting function in mitochondria (Chew *et al.*, 2003); therefore, the roles of the transit peptide in stroma APX need further verification. Numerous studies of ROS-scavenging enzymes have proved that APX activity increases under heat stress (Sato *et al.*, 2001; Ma *et al.*, 2008; Kim *et al.*, 2010). However, the different characteristics of APX isoenzymes (Nakano and Asada, 1981; Asada, 1992) imply that they potentially have specific functions under stress conditions. Cytosolic APX isoenzymes (cAPX) are considered to be sensitive and responsible for adaptation to environmental changes. Induction of *cAPX* gene under environmental stresses has been intensively studied in *Arabidopsis*. Normally, only *cAPX1* is constitutively expressed (Santos *et al.*, 1996) and *cAPX2* is significantly induced under stress conditions (Fryer *et al.*, 2003; Chang *et al.*, 2004). APX2 is thermostable and compensates for APX1 under heat stress (Panchuk *et al.*, 2002). In CG, expressions of *PpcAPX2* and *PpcAPX3* were significantly induced, whereas *PpcAPX1* was maintained at a steady level, in response to chronic heat stress (Fig. 10a). However, the inducible expressions of *PpcAPX2* and *PpcAPX3* were limited in WH, and the expression of *PpcAPX1* was even inhibited under chronic heat stress (Fig. 10b). The inducible expressions of peroxisomal and chloroplastic *APX* genes under chronic heat stress seemed to be related to that of cytosolic APX. When the cytoslic *APX* gene was significantly induced, the expression levels of *PppAPX*, *PpsAPX*, and *PptAPX* were also maintained at a high level in CG (Fig. 10a), but showed the opposite trend in WH (Fig. 10b). The interrelationship of APX isoenzymes has been proven in *Arabidopsis*, in which the H_2O_2-scavenging system in chloroplasts totally collapses when *cAPX1* is knocked out (Davletova *et al.*, 2005). However, despite significant induction of *cAPX* in response to oxidative stresses, transcript levels of chloroplastic and peroxisomal APX isoenzymes are unchanged, and chloroplastic APX activities even decrease under strong light conditions (Yoshimura *et al.*, 2000). This contradictory result can be explained as follows. Specific expression of *APX* genes is genotype-dependent under environmental stress. For example,

in wheat cytosolic *APXII* and thylakoid *APX* genes are significantly up-regulated in a drought-tolerant cultivar, and cytosolic *APXI* and stroma *APXII* genes are increased in a drought-sensitive cultivar, but APX activity increases only in the drought-tolerant genotype (Sečenji *et al.*, 2009), because chloroplastic APX activity is rapidly inactivated especially in the absence of ascorbate (Miyake and Asada, 1996). The crystal structure of stromal APX shows a unique loop in the vicinity of the heme that is related to the stability of chloroplastic APX, whereas no specific loop is present in cAPX (Martinez *et al.*, 1994; Kitajima *et al.*, 2006). A specific structure and complex regulatory mechanism at the transcriptional or post-transcriptional level result in different antioxidant capacities under oxidative stresses.

In the present study, the transcript patterns of *APX* genes in two pear cultivars indicate that CG shows better adaptability to chronic heat stress and that induction of cytosolic *APX* plays an important role in the thermal adaptability of CG.

Acknowledgements

We thank Prof. Xue-ping ZHOU, Institute of Biotechnology, Zhejiang University, China, for kindly providing the pCHF3-GFP plastid.

Compliance with ethics guidelines

Dong-feng LIU, Dong ZHANG, Guo-qin LIU, Sayed HUSSAIN, and Yuan-wen TENG declare that they have no conflict of interest.

This article does not contain any studies with human or animal subjects performed by any of the authors.

References

Apel, K., Hirt, H., 2004. Reactive oxygen species: metabolism, oxidative stress, and signal transduction. *Annu. Rev. Plant Biol.*, **55**(1):373-399. [doi:10.1146/annurev.arplant.55.031903.141701]

Aro, E.M., Suorsa, M., Rokka, A., Allahverdiyeva, Y., Paakkarinen, V., Saleem, A., Battchikova, N., Rintamäki, E., 2005. Dynamics of photosystem II: a proteomic approach to thylakoid protein complexes. *J. Exp. Bot.*, **56**(411):347-356. [doi:10.1093/jxb/eri041]

Asada, K., 1992. Ascorbate peroxidase—a hydrogen peroxide-scavenging enzyme in plants. *Physiol. Plantarum*, **85**(2):235-241. [doi:10.1111/j.1399-3054.1992.tb04728.x]

Asada, K., 1999. The water-water cycle in chloroplasts: scavenging of active oxygen and dissipation of excess photons. *Annu. Rev. Plant Physiol. Plant Mol. Biol.*, **50**(1):601-639. [doi:10.1146/annurev.arplant.50.1.601]

Asada, K., 2006. Production and scavenging of reactive oxygen species in chloroplasts and their functions. *Plant Physiol.*, **141**(2):391-396. [doi:10.1104/pp.106.082040]

Bienert, G.P., Møller, A.L.B., Kristiansen, K.A., Schulz, A., Møller, I.M., Schjoerring, J.K., Jahn, T.P., 2007. Specific aquaporins facilitate the diffusion of hydrogen peroxide across membranes. *J. Biol. Chem.*, **282**(2):1183-1192. [doi:10.1074/jbc.M603761200]

Bohnert, H.J., Nelson, D.E., Jensen, R.G., 1995. Adaptations to environment stresses. *Plant Cell*, **7**(7):1099-1111. [doi:10.2307/3870060]

Chang, C.C.C., Ball, L., Fryer, M.J., Baker, N.R., Karpinski, S., Mullineaux, P.M., 2004. Induction of ascorbate peroxidase 2 expression in wounded *Arabidopsis* leaves does not involve known wound-signalling pathways but is associated with changes in photosynthesis. *Plant J.*, **38**(3):499-511. [doi:10.1111/j.1365-313X.2004.02066.x]

Chew, O., Whelan, J., Millar, A.H., 2003. Molecular definition of the ascorbate-glutathione cycle in *Arabidopsis* mitochondria reveals dual targeting of antioxidant defenses in plants. *J. Biol. Chem.*, **278**(47):46869-46877. [doi:10.1074/jbc.M307525200]

Crafts-Brandner, S.J., Salvucci, M.E., 2002. Sensitivity of photosynthesis in a C4 plant, maize, to heat stress. *Plant Physiol.*, **129**(4):1773-1780. [doi:10.1104/pp.002170]

Dat, J., Vandenabeele, S., Vranová, E., van Montagu, M., Inzé, D., van Breusegem, F., 2000. Dual action of the active oxygen species during plant stress responses. *Cell. Mol. Life Sci.*, **57**(5):779-795. [doi:10.1007/s000180050041]

Davletova, S., Rizhsky, L., Liang, H., Shengqiang, Z., Oliver, D.J., Coutu, J., Shulaev, V., Schlauch, K., Mittler, R., 2005. Cytosolic ascorbate peroxidase 1 is a central component of the reactive oxygen gene network of *Arabidopsis*. *Plant Cell*, **17**(1):268-281. [doi:10.1105/tpc.104.026971]

Foyer, C.H., Lelandais, M., Kunert, K.J., 1994. Photooxidative stress in plants. *Physiol. Plantarum*, **92**(4):696-717. [doi:10.1111/j.1399-3054.1994.tb03042.x]

Fridovich, I., 1998. Oxygen toxicity: a radical explanation. *J. Exp. Biol.*, **201**(8):1203-1209.

Fryer, M.J., Ball, L., Oxborough, K., Karpinski, S., Mullineaux, P.M., Baker, N.R., 2003. Control of ascorbate peroxidase 2 expression by hydrogen peroxide and leaf water status during excess light stress reveals a functional organisation of *Arabidopsis* leaves. *Plant J.*, **33**(4):691-705. [doi:10.1046/j.1365-313X.2003.01656.x]

Glenn, D.M., Prado, E., Erez, A., Mcferson, J., Puterka, G.J., 2002. A reflective, processed-kaolin particle film affects fruit temperature, radiation reflection, and solar injury in apple. *J. Am. Soc. Hortic. Sci.*, **127**(2):188-193.

Havaux, M., 1993. Rapid photosynthetic adaptation to heat

stress triggered in potato leaves by moderately elevated temperatures. *Plant Cell Environ*., **16**(4):461-467. [doi:10.1111/j.1365-3040.1993.tb00893.x]

Heath, R.L., Packer, L., 1968. Photoperoxidation in isolated chloroplasts: I. Kinetics and stoichiometry of fatty acid peroxidation. *Arch. Biochem. Biophys*., **125**(1):189-198. [doi:10.1016/0003-9861(68)90654-1]

Huang, X.Z., Chen, Y.T., Lei, Y., Cai, S.H., Chen, X.M., 2010. Causes and control strategies of a large number of early falling leaves of pear in Fujian. *Chin. Agric. Sci. Bull*., **26**(2):91-95 (in Chinese).

Ishikawa, T., Shigeoka, S., 2008. Recent advances in ascorbate biosynthesis and the physiological significance of ascorbate peroxidase in photosynthesizing organisms. *Biosci. Biotechnol. Biochem*., **72**(5):1143-1154. [doi:10.1271/bbb.80062]

Ishikawa, T., Yoshimura, K., Tamoi, M., Takeda, T., Shigeoka, S., 1997. Alternative mRNA splicing of 3′-terminal exons generates ascorbate peroxidase isoenzymes in spinach (*Spinacia oleracea*) chloroplasts. *Biochem. J.*, **328**(Pt 3):795-800.

Ishikawa, T., Yoshimura, K., Sakai, K., Tamoi, M., Takeda, T., Shigeoka, S., 1998. Molecular characterization and physiological role of a glyoxysome-bound ascorbate peroxidase from spinach. *Plant Cell Physiol*., **39**(1):23-34. [doi:10.1093/oxfordjournals.pcp.a029285]

Ji, W.W., Qiu, C.H., Jiao, Y., Guo, Y.P., Teng, Y.W., 2012. Effects of high temperature and strong light on photosynthesis, D1 protein, and the Deg1 protease in pear (*Pyrus pyrifolia*) leaves. *J. Fruit Sci*., **29**(5):794-799.

Jimenez, A., Hernandez, J.A., Del Rio, L.A., Sevilla, F., 1997. Evidence for the presence of the ascorbate-glutathione cycle in mitochondria and peroxisomes of pea leaves. *Plant Physiol*., **114**(1):275-284. [doi:10.1104/pp.114.1.275]

Karpinski, S., Reynolds, H., Karpinska, B., Wingsle, G., Creissen, G., Mullineaux, P., 1999. Systemic signaling and acclimation in response to excess excitation energy in *Arabidopsis*. *Science*, **284**(5414):654-657. [doi:10.1126/science.284.5414.654]

Kim, M.D., Kim, Y.H., Kwon, S.Y., Yun, D.J., Kwak, S.S., Lee, H.S., 2010. Enhanced tolerance to methyl viologen-induced oxidative stress and high temperature in transgenic potato plants overexpressing the *CuZnSOD*, *APX* and *NDPK2* genes. *Physiol. Plant.*, **140**(2):153-162. [doi:10.1111/j.1399-3054.2010.01392.x]

Kitajima, S., Tomizawa, K.I., Shigeoka, S., Yokota, A., 2006. An inserted loop region of stromal ascorbate peroxidase is involved in its hydrogen peroxide-mediated inactivation. *FEBS J*., **273**(12):2704-2710. [doi:10.1111/j.1742-4658.2006.05286.x]

Kratsch, H.A., Wise, R.R., 2000. The ultrastructure of chilling stress. *Plant Cell Environ*., **23**(4):337-350. [doi:10.1046/j.1365-3040.2000.00560.x]

Krause, G., Weis, E., 1984. Chlorophyll fluorescence as a tool in plant physiology. *Photosynth. Res*., **5**(2):139-157. [doi:10.1007/BF00028527]

Law, R.D., Crafts-Brandner, S.J., 1999. Inhibition and acclimation of photosynthesis to heat stress is closely correlated with activation of ribulose-1,5-bisphosphate carboxylase/oxygenase. *Plant Physiol*., **120**(1):173-182. [doi:10.1104/pp.120.1.173]

Li, P.M., Cheng, L.L., 2009. The elevated anthocyanin level in the shaded peel of 'anjou' pear enhances its tolerance to high temperature under high light. *Plant Sci*., **177**(5):418-426. [doi:10.1016/j.plantsci.2009.07.005]

Liu, G., Li, W., Zheng, P., Xu, T., Chen, L., Liu, D., Hussain, S., Teng, Y., 2012. Transcriptomic analysis of 'suli' pear (*Pyrus pyrifolia* white pear group) buds during the dormancy by RNA-Seq. *BMC Genomics*, **13**(1):700. [doi:10.1186/1471-2164-13-700]

Livak, K.J., Schmittgen, T.D., 2001. Analysis of relative gene expression data using real-time quantitative PCR and the $2^{-\Delta\Delta C_T}$ method. *Methods*, **25**(4):402-408. [doi:10.1006/meth.2001.1262]

Ma, Y.H., Ma, F.W., Zhang, J.K., Li, M.J., Wang, Y.H., Liang, D., 2008. Effects of high temperature on activities and gene expression of enzymes involved in ascorbate-glutathione cycle in apple leaves. *Plant Sci*., **175**(6):761-766. [doi:10.1016/j.plantsci.2008.07.010]

Martinez, S.E., Huang, D., Szczepaniak, A., Cramer, W.A., Smith, J.L., 1994. Crystal structure of chloroplast cytochrome reveals a novel cytochrome fold and unexpected heme ligation. *Structure*, **2**(2):95-105. [doi:10.1016/S0969-2126(00)00012-5]

Mittler, R., 2002. Oxidative stress antioxidantandstress tolerance. *Trends Plant Sci.*, **7**(9):405-410. [doi:10.1016/S1360-1385(02)02312-9]

Mittler, R., Zilinskas, B.A., 1992. Molecular cloning and characterization of a gene encoding pea cytosolic ascorbate peroxidase. *J. Biol. Chem.*, **267**(30):21802-21807.

Mittler, R., Vanderauwera, S., Gollery, M., van Breusegem, F., 2004. Reactive oxygen gene network of plants. *Trends Plant Sci*., **9**(10):490-498. [doi:10.1016/j.tplants.2004.08.009]

Miyake, C., Asada, K., 1996. Inactivation mechanism of ascorbate peroxidase at low concentrations of ascorbate; hydrogen peroxide decomposes compound I of ascorbate peroxidase. *Plant Cell Physiol*., **37**(4):423-430. [doi:10.1093/oxfordjournals.pcp.a028963]

Mullineaux, P.M., 2006. Spatial dependence for hydrogen peroxide-directed signaling in light-stressed plants. *Plant Physiol*., **141**(2):346-350. [doi:10.1104/pp.106.078162]

Najami, N., Janda, T., Barriah, W., Kayam, G., Tal, M., Guy, M., Volokita, M., 2008. Ascorbate peroxidase gene family in tomato: its identification and characterization. *Mol. Genet. Genomics*, **279**(2):171-182. [doi:10.1007/s00438-007-0305-2]

Nakano, Y., Asada, K., 1981. Hydrogen peroxide is scavenged by ascorbate-specific peroxidase in spinach chloroplasts. *Plant Cell Physiol*., **22**(5):867-880.

Neill, S., Desikan, R., Hancock, J., 2002. Hydrogen peroxide signalling. *Curr. Opin. Plant Biol*., **5**(5):388-395. [doi:10.1016/S1369-5266(02)00282-0]

Panchuk, I.I., Volkov, R.A., Schöffl, F., 2002. Heat stress- and

heat shock transcription factor-dependent expression and activity of ascorbate peroxidase in *Arabidopsis*. *Plant Physiol*., **129**(2):838-853. [doi:10.1104/pp.001362]

Santos, M., Gousseau, H., Lister, C., Foyer, C., Creissen, G., Mullineaux, P., 1996. Cytosolic ascorbate peroxidase from *Arabidopsis thaliana* L. is encoded by a small multigene family. *Planta*, **198**(1):64-69. [doi:10.1007/BF00197587]

Sato, Y., Murakami, T., Funatsuki, H., Matsuba, S., Saruyama, H., Tanida, M., 2001. Heat shock-mediated *APX* gene expression and protection against chilling injury in rice seedlings. *J. Exp. Bot*., **52**(354):145-151. [doi:10.1093/jexbot/52.354.145]

Sečenji, M., Hideg, E., Bebes, A., Györgyey, J., 2009. Transcriptional differences in gene families of the ascorbate-glutathione cycle in wheat during mild water deficit. *Plant Cell Rep*., **29**(1):37-50. [doi:10.1007/s00299-009-0796-x]

Shigeoka, S., Ishikawa, T., Tamoi, M., Miyagawa, Y., Takeda, T., Yabuta, Y., Yoshimura, K., 2002. Regulation and function of ascorbate peroxidase isoenzymes. *J. Exp. Bot*., **53**(372):1305-1319. [doi:10.1093/jexbot/53.372.1305]

Sparkes, I.A., Runions, J., Kearns, A., Hawes, C., 2006. Rapid, transient expression of fluorescent fusion proteins in tobacco plants and generation of stably transformed plants. *Nat. Protoc.*, **1**(4):2019-2025. [doi:10.1038/nprot.2006.286]

Teixeira, F., Menezes-Benavente, L., Margis, R., Margis-Pinheiro, M., 2004. Analysis of the molecular evolutionary history of the ascorbate peroxidase gene family: inferences from the rice genome. *J. Mol. Evol*., **59**(6):761-770. [doi:10.1007/s00239-004-2666-z]

Teixeira, F., Menezes-Benavente, L., Galvão, V., Margis, R., Margis-Pinheiro, M., 2006. Rice ascorbate peroxidase gene family encodes functionally diverse isoforms localized in different subcellular compartments. *Planta*, **224**(2):300-314. [doi:10.1007/s00425-005-0214-8]

Vandenabeele, S., van der Kelen, K., Dat, J., Gadjev, I., Boonefaes, T., Morsa, S., Rottiers, P., Slooten, L., van Montagu, M., Zabeau, M., *et al.*, 2003. A comprehensive analysis of hydrogen peroxide-induced gene expression in tobacco. *PNAS*, **100**(26):16113-16118. [doi:10.1073/pnas.2136610100]

Vanderauwera, S., Suzuki, N., Miller, G., van de Cotte, B., Morsa, S., Ravanat, J.L., Hegie, A., Triantaphylidès, C., Shulaev, V., van Montagu, M.C.E., *et al.*, 2011. Extranuclear protection of chromosomal DNA from oxidative stress. *PNAS*, **108**(4):1711-1716. [doi:10.1073/pnas.1018359108]

Volkov, R., Panchuk, I., Mullineaux, P., Schoffl, F., 2006. Heat stress-induced H_2O_2 is required for effective expression of heat shock genes in *Arabidopsis*. *Plant Mol. Biol*., **61**(4-5):733-746. [doi:10.1007/s11103-006-0045-4]

Wang, J., Ou, Y., Wu, Z., Dai, L.Z., Liu, S.W., 2011. Effects of high temperature stress on physiological indicators, early defoliation of early-maturing pear. *Southwest China J. Agric. Sci.*, **24**(2):546-551 (in Chinese).

Yamamoto, Y., Aminaka, R., Yoshioka, M., Khatoon, M., Komayama, K., Takenaka, D., Yamashita, A., Nijo, N., Inagawa, K., Morita, N., *et al.*, 2008. Quality control of photosystem II: impact of light and heat stresses. *Photosynth. Res*., **98**(1-3):589-608. [doi:10.1007/s11120-008-9372-4]

Yoshimura, K., Yabuta, Y., Ishikawa, T., Shigeoka, S., 2000. Expression of spinach ascorbate peroxidase isoenzymes in response to oxidative stresses. *Plant Physiol*., **123**(1):223-234. [doi:10.1104/pp.123.1.223]

Yu, B., Zhang, D., Huang, C., Qian, M., Zheng, X., Teng, Y., Su, J., Shu, Q., 2012. Isolation of anthocyanin biosynthetic genes in red Chinese sand pear (*Pyrus pyrifolia* Nakai) and their expression as affected by organ/tissue, cultivar, bagging and fruit side. *Sci. Hort*., **136**:29-37. [doi:10.1016/j.scienta.2011.12.026]